

Power Controllability of a Three-Phase Converter with an Unbalanced AC Source

S.Sujith Kumar

Pursuing M.Tech, PE Branch,
Dept of EEE,

Vinuthna Institute of Technology Science, Warangal.

M.Shireesha

Associate Professor,
Dept of EEE,

Vinuthna Institute of Technology Science, Warangal.

Abstract:

Three-phase dc–ac power converters suffer from power oscillation and overcurrent problems in case of the unbalanced ac source voltage that can be caused by grid/generator faults. Existing solutions to handle these problems are properly selecting and controlling the positive- and negative-sequence currents. In this paper, a new series of control strategies which utilize the zero- sequence components are proposed to enhance the power control ability under this adverse condition. It is concluded that by introducing proper zero-sequence current controls and corresponding circuit configurations, the power converter can enable more flexible control targets, achieving better performances in the delivered power and the load current when suffering from the unbalanced ac voltage.

Index Terms:

Control strategy, dc–ac converter, fault tolerance, unbalanced ac source.

I. INTRODUCTION:

In many important applications for power electronics such as renewable energy generation, motor drives, power quality, and microgrid, etc., the three-phase dc–ac converters are critical components as the power flow interface of dc and ac electrical systems [1], [2]. As shown in Fig. 1, a dc–ac voltage source converter with a corresponding filter is typically used to convert the energy between the dc bus and the three-phase ac sources, which could be the power grid, generation units, or the electric machines depending on the applications and controls [3]–[5].

Since the power electronics are getting so widely used and becoming essential in the energy conversion technology, the failures or shutting down of these backbone dc–ac converters may result in serious problems and cost. It is becoming a need in many applications that the power converters should be reliable to withstand some faults or disturbances in order to ensure certain availability of the energy supply [6]–[13]. A good example can be seen in the wind power application, where both the total installed capacity and individual capacity of the power conversion system are relatively high. The sudden disconnection of the power converter may cause significant impacts on the grid stability and also on the high cost for maintenance/repair [1]. As a result, transmission system operators (TSOs) in different countries have been issuing strict requirements for the wind turbine behavior under grid faults. As shown in Fig. 2, the wind power converter should be connected (or even keep generating power) under various grid voltage dips for certain time according to the dip severity, and in some uncritical conditions (e.g., 90% voltage dip), the power converter may need long-time operation [1], [2], [12], [13].

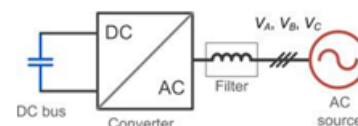


Fig. 1. Typical dc–ac power

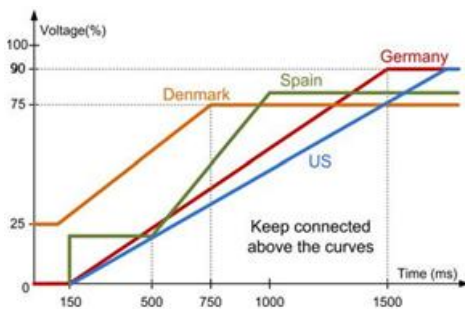


Fig. 2. Grid codes of wind turbines under the grid voltage dip by different countries.

When the ac source shown in Fig. 1 becomes distorted under faults or disturbances, the unbalanced ac voltages have been proven to be one of the greatest challenges for the control of the dc-ac converter in order to keep them normally operating and connected to the ac source [2], [14], [15]. Special control methods which can regulate both the positive- and negative-sequence currents have been introduced to handle these problems [2], [16]–[21]. However, the resulting performances by these control methods seem to be still not satisfactory: either distorted load currents or power oscillations will be presented, and thereby not only the ac source but also the power converter will be further stressed accompanying with the costly design considerations.

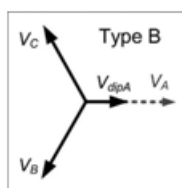


Fig. 3. Phasor diagram definitions for the voltage dips in the ac source of Fig. 1. V_A , V_B , and V_C means the voltage of three phases in the ac source.

This paper targets to understand and improve the power control limits of a typical three-phase dc-ac converter system under the unbalanced ac source. A new series of control strategies which utilizes the zero-sequence components are then proposed to enhance the power control ability under this adverse condition.

Besides the grid integration, the proposed control methods have the potential to be applied under other applications like the motor/generator connections or microgrids, where the un-balanced ac voltage is likely to be presented; therefore, the basic principle and feasibility are mainly focused.

II. LIMITS OF A TYPICAL THREE-WIRE CONVERTER SYSTEM

In order to analyze the controllability and the performance of the power electronics converter under an adverse ac source, a severe unbalanced ac voltage is first defined as a case study in this paper. As shown in Fig. 3, the phasor diagram of the three-phase distorted ac voltage are indicated, it is assumed that the type B fault happens with the significant voltage dip on phase A of the ac source. Also, there are many other types of voltage faults which have been defined as type A–F in [22]. According to [2] and [19], any distorted three-phase voltage can be expressed by the sum of components in the positive sequence, negative sequence, and zero sequence. For simplicity of analysis, only the components with the fundamental frequency are considered in this paper, however, it is also possible to extend the analysis to higher order harmonics. The distorted three-phase ac source voltage in Fig. 3 can be represented by

$$\begin{aligned}
 \mathbf{V}_S &= \mathbf{V}^+ + \mathbf{V}^- + \mathbf{V}^0 \\
 &= \begin{bmatrix} v_a \\ v_b \\ v_c \end{bmatrix} = V^+ \begin{bmatrix} \sin(\omega t + \varphi^+) \\ \sin(\omega t - 120^\circ + \varphi^+) \\ \sin(\omega t + 120^\circ + \varphi^+) \end{bmatrix} \\
 &\quad + V^- \begin{bmatrix} \sin(\omega t + \varphi^-) \\ \sin(\omega t + 120^\circ + \varphi^-) \\ \sin(\omega t - 120^\circ + \varphi^-) \end{bmatrix} + V^0 \begin{bmatrix} \sin(\omega t + \varphi^0) \\ \sin(\omega t + \varphi^0) \\ \sin(\omega t + \varphi^0) \end{bmatrix} \quad (1)
 \end{aligned}$$

where V^+ , V^- , and V^0 are the voltage amplitude in the positive, negative, and zero sequence, respectively. And ϕ^+ , ϕ^- , and ϕ^0 represent the initial phase angles in the positive sequence, negative sequence, and zero sequence, respectively. The predefined voltage dip as indicated in Fig. 3 should contain voltage components in all the three sequences [2], [11].

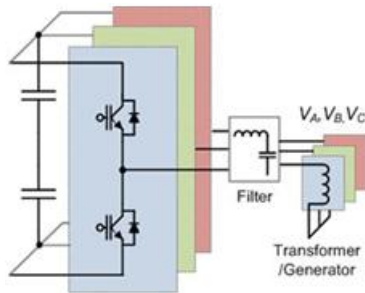


Fig. 4. Typical three-phase three-wire 2L-voltage source converter.

TABLE I: CONVERTER PARAMETERS FOR THE CASE STUDY

Rated output active power P_o	10 MW
DC bus voltage V_{dc}	5.6 kV DC
*Rated primary side voltage V_p	3.3 kV rms
Rated line-to-line grid voltage V_g	20 kV rms
Rated load current I_{load}	1.75 kA rms
Carrier frequency f_c	750 Hz
Filter inductance L_f	1.1 mH (0.25 p.u.)

*Line-to-line voltage in the primary windings of transformer.

A typically used three-phase three-wire two-level voltage source dc–ac converter is chosen and basically designed, as shown in Fig. 4 and Table I, where the converter configuration and the parameters are indicated, respectively. It is noted that the three-phase ac source is represented here by three windings with a common neutral point, which can be the windings of an electric machine or a transformer. Because there are only three wires and a common neutral point in the windings of the ac source, the currents flowing in the three phases do not contain zero-sequence components. As a result, the three-phase load current controlled by the converter can be written as

$$I_C = I^+ + I^- \quad (2)$$

With the voltage of the ac source in (1) and the current controlled by the converter in (2), the instantaneous real power p and the imaginary power q in $\alpha\beta$ coordinate, as well as the real power p_0 in the zero coordinate can be calculated as

$$\begin{bmatrix} p \\ q \\ p_0 \end{bmatrix} = \begin{bmatrix} v_\alpha \cdot i_\alpha + v_\beta \cdot i_\beta \\ v_\alpha \cdot i_\beta - v_\beta \cdot i_\alpha \\ v_0 \cdot 0 \end{bmatrix} = \begin{bmatrix} \bar{P} + P_{c2} \cdot \cos(2\omega t) + P_{s2} \cdot \sin(2\omega t) \\ \bar{Q} + Q_{c2} \cdot \cos(2\omega t) + Q_{s2} \cdot \sin(2\omega t) \\ 0 \end{bmatrix} \quad (3)$$

Then, the instantaneous three-phase real power $p_{3\phi}$ and the imaginary power $q_{3\phi}$ of the ac source/converter can be written

$$\begin{bmatrix} p_{3\phi} \\ q_{3\phi} \end{bmatrix} = \begin{bmatrix} p + p_0 \\ q \end{bmatrix} = \begin{bmatrix} \bar{P} \\ \bar{Q} \end{bmatrix} + \begin{bmatrix} P_{c2} \\ Q_{c2} \end{bmatrix} \cos(2\omega t) + \begin{bmatrix} P_{s2} \\ Q_{s2} \end{bmatrix} \sin(2\omega t) \quad (4)$$

where \bar{P} and \bar{Q} are the average parts of the real and imaginary power, P_{c2} , P_{s2} and Q_{c2} , Q_{s2} are the oscillation parts, which can be calculated as

$$\begin{aligned} \bar{P} &= \frac{3}{2}(v_d^+ \cdot i_d^+ + v_q^+ \cdot i_q^+ + v_d^- \cdot i_d^- + v_q^- \cdot i_q^-) \\ P_{c2} &= \frac{3}{2}(v_d^- \cdot i_d^+ + v_q^- \cdot i_q^+ + v_d^+ \cdot i_d^- + v_q^+ \cdot i_q^-) \\ P_{s2} &= \frac{3}{2}(v_q^- \cdot i_d^+ - v_d^- \cdot i_q^+ - v_q^+ \cdot i_d^- + v_d^+ \cdot i_q^-) \\ \bar{Q} &= \frac{3}{2}(v_q^+ \cdot i_d^+ - v_d^+ \cdot i_q^+ + v_q^- \cdot i_d^- - v_d^- \cdot i_q^-) \\ Q_{c2} &= \frac{3}{2}(v_q^- \cdot i_d^+ - v_d^- \cdot i_q^+ + v_q^+ \cdot i_d^- - v_d^+ \cdot i_q^-) \\ Q_{s2} &= \frac{3}{2}(-v_d^- \cdot i_d^+ - v_q^- \cdot i_q^+ + v_d^+ \cdot i_d^- + v_q^+ \cdot i_q^-) \end{aligned} \quad (5)$$

where a positive dq synchronous reference frame and a negative dq synchronous reference frame are applied, respectively, to the positive- and negative-sequence voltage/current. Each of the components on the corresponding positive- and negative-dq axis can be written as

$$\begin{aligned} v_d^+ &= V^+ \cos(\varphi^+) \\ v_q^+ &= V^+ \sin(\varphi^+) \\ v_d^- &= V^- \cos(\varphi^-) \\ v_q^- &= -V^- \sin(\varphi^-) \end{aligned} \quad (7)$$

$$\begin{aligned} i_d^+ &= I^+ \cos(\delta^+) \\ i_q^+ &= I^+ \sin(\delta^+) \\ i_d^- &= I^- \cos(\delta^-) \\ i_q^- &= -I^- \sin(\delta^-) \end{aligned} \quad (8)$$

Then, (5) and (6) can be formulated as a matrix relation as

$$\begin{bmatrix} \bar{P} \\ \bar{Q} \\ P_{e2} \\ P_{e2} \end{bmatrix} = \frac{3}{2} \begin{bmatrix} v_d^+ & v_q^+ & v_d^- & v_q^- \\ v_q^+ & -v_d^+ & v_q^- & -v_d^- \\ v_q^- & -v_d^- & -v_q^+ & v_d^+ \\ v_d^- & v_q^- & v_d^+ & v_q^+ \end{bmatrix} \begin{bmatrix} i_d^+ \\ i_q^+ \\ i_d^- \\ i_q^- \end{bmatrix} \quad (9)$$

It can be seen from (9) that if the ac source voltage is decided, then the converter has four controllable freedoms (i_d^+ , i_q^+ , i_d^- , and i_q^-) to regulate the current flowing in the ac source. That also means: four control targets/functions can be established. delivered by the converter are two basic requirements for a given application, then, two control targets have to be first settled as

$$\bar{P}_{sp} = \bar{P} = P_{ref} \quad (10)$$

$\bar{Q}_{sp} = \bar{Q} = Q_{ref}$
It is noted that different applications may have different re-

It is noted that different applications may have different requirements for the control of the average power, e.g., in the power production application, the active power reference P_{ref} injected to the grid is normally set as positive, meanwhile the large amount of the reactive power Q_{ref} may be needed in order to help to support the grid voltage [12], [13]. As for the electric machine application, the P_{ref} is set as negative for the generator mode and positive for the motor mode, there may be no or just a few reactive power Q_{ref} requirements for magnetizing of the electric machine. While in most power quality applications, e.g., STACOM, P_{ref} is normally set to be very small to provide the converter loss, and a large amount of Q_{ref} is normally required. Consequently, for the three-phase three-wire converter system, there are only two more current control freedoms left to achieve another two control targets besides (10). These two adding control targets may be utilized to further improve the performances of the converter under the unbalanced ac source, which have been generally investigated in [2] and [16]–[18]. However, this paper focuses more on the evaluation of control limits and the control possibilities under the whole voltage dipping range.

In the following, two of the most mentioned control methods achieved by three-wire converter structure are investigated under the unbalanced ac source.

A. Elimination of the Negative-Sequence Current

In most of the grid integration applications, there are strict grid codes to regulate the behavior of the grid connected converters. The negative-sequence current which always results in the unbalanced load current may be unacceptable from the point view of a TSO [13]. Therefore, extra two control targets which aim to eliminate the negative-sequence current can be added as

$$\begin{aligned} i_d^- &= 0 \\ i_q^- &= 0. \end{aligned} \quad (11)$$

Translating the control targets in (10) and (11), all the controllable current components can be calculated as

$$\begin{aligned} i_d^+ &= \frac{2}{3} \cdot \frac{v_d^+ \cdot P_{ref} + v_q^+ \cdot Q_{ref}}{(v_d^+)^2 - (v_d^-)^2} \\ i_q^+ &= \frac{2}{3} \cdot \frac{P_{ref}}{v_d^+} - \frac{v_d^-}{v_q^+} \cdot i_d^+ \end{aligned} \quad (12)$$

$$\begin{aligned} i_d^- &= 0 \\ i_q^- &= 0. \end{aligned} \quad (13)$$

When applying the current references in (12) and (13), the ac source voltage, load current, sequence current amplitude, and the instantaneous power delivered by the converter are shown in Fig. 5. The simulation is based on the parameters predefined Normally, the three-phase average active and reactive powers

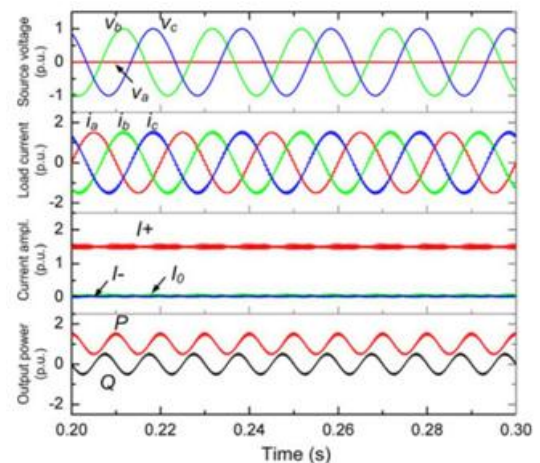


Fig. 5. Simulation of the converter with no negative-sequence current control (three-phase three-wire converter, $P_{ref} = 1$ p.u., $Q_{ref} = 0$ p.u., $I_d^- = 0$ p.u., $I_q^- = 0$ p.u., $V_A = 0$ p.u., I_+ , I_- , and I_0 means the amplitude of the current in the positive, negative, and zero sequences, respectively).

Dipping to zero. The average active power reference P_{ref} for the converter is set as 1 p.u. and the reactive power reference Q_{ref} is set as 0. It can be seen from Fig. 5 that with the extra control targets in (11), there is no zero-sequence nor negative-sequence components in the load current, i.e., the currents among the three phases of converter are symmetrical under the given unbalanced ac source condition. The current amplitude in different sequences and the delivered active/reactive power with relation to the voltage amplitude of the dipping phase V_A are shown in Fig. 6(a) and (b), respectively. It is noted that only the positive-sequence current is generated by the converter, and there is up to ± 0.5 p.u. oscillations both in the active and reactive power when V_A dips to zero. The significant fluctuation of the active power would result in the voltage fluctuation of the dc bus [16]–[19], compromising not only the THD but also the reliability performances of the converter according to [23].

B. Elimination of the Active Power Oscillation

In order to overcome the disadvantage of the active power oscillation under the unbalanced ac source, another two extra control targets which aim to cancel the oscillation items in the instantaneous active power can be used to replace (11) as

$$\begin{aligned} P_{3\phi c2} &= P_{c2} = 0 \\ P_{3\phi s2} &= P_{s2} = 0. \end{aligned} \quad (14)$$

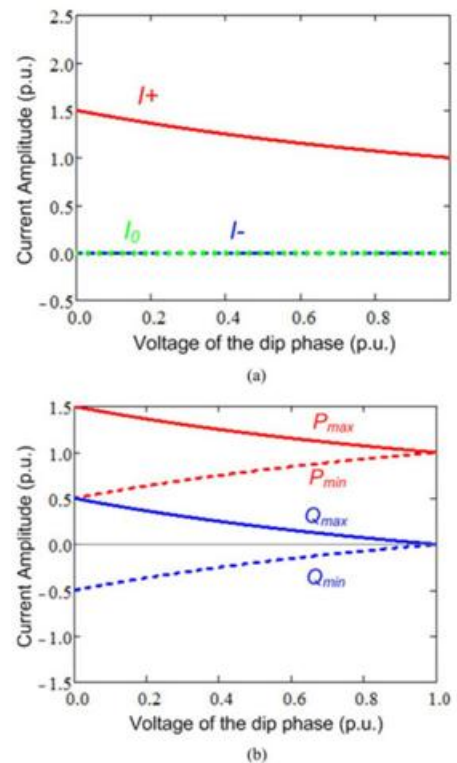


Fig. 6. Profile of converter control with no negative-sequence current (three-phase three-wire converter, $P_{ref} = 1$ p.u., $Q_{ref} = 0$ p.u., $I_d^- = 0$ p.u., $I_q^- = 0$ p.u.). (a) Sequence current amplitude versus V_A (I_+ , I_- , and I_0 means the amplitude of the current in the positive, negative, and zero sequences, respectively). (b) P and Q oscillation range versus V_A .

Then, according to (9), each of the current components can be calculated as

$$\begin{aligned} \begin{bmatrix} i_d^+ \\ i_q^+ \\ i_d^- \\ i_q^- \end{bmatrix} &= \frac{2}{3} \begin{bmatrix} v_d^+ & v_q^+ & v_d^- & v_q^- \\ v_q^+ & -v_d^+ & v_q^- & -v_d^- \\ v_q^- & -v_d^- & -v_q^+ & v_d^+ \\ v_d^- & v_q^- & v_d^+ & v_q^+ \end{bmatrix}^{-1} \begin{bmatrix} P_{ref} \\ 0 \\ 0 \\ 0 \end{bmatrix} \\ &= \frac{2P_{ref}}{3M} \begin{bmatrix} v_d^+ \\ v_q^+ \\ -v_d^- \\ -v_q^- \end{bmatrix} \end{aligned} \quad (15)$$

where

$$M = (v_d^+)^2 + (v_q^+)^2 - (v_d^-)^2 - (v_q^-)^2. \quad (16)$$

When applying the current references in (15), the corresponding source voltage, load current, sequence current, and the instantaneous power delivered by the converter are shown in Fig. 7

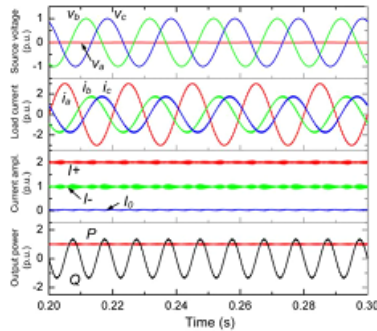


Fig. 7. Simulation of the converter control with no active power oscillation (three-phase three-wire converter, Pref = 1 p.u., Qref = 0 p.u., Ps2 = 0 p.u., Pc2 = 0 p.u., VA = 0 p.u. I+, I-, and I0 means the amplitude of the current in the positive, negative, and zero sequences, respectively.

It can be seen that the active power oscillation at twice of the fundamental frequency can be eliminated. However, the disadvantage of this control strategy is also significant: first, the converter has to deliver up to 3 p.u. load current in the faulty phase which is much larger than the currents in other two normal phases—this large current may cause over loading of the system and result in failures. Moreover, significant fluctuation of the reactive power will be presented compared to the control strategy in Fig. 5. In case of the grid-connected application, this significant reactive power oscillation may cause grid voltage fluctuation, which is unpreferred especially with weak grid and grid faults. The current amplitude in the different sequences, as well as the delivered active/reactive power with relation to the voltage amplitude on the dipping phase is shown in Fig. 8(a) and (b), respectively. It is noted that the converter has to deliver both the positive- and negative-sequence current to achieve this control strategy, and up to ±1.3 p.u. oscillation in the reactive power is generated when VA dips to zero. Another three possible control strategies which can eliminate the oscillation of the reactive power as shown in (17)

or reduce the oscillations of both active and reactive power as shown in (18) and (19), are also possible for the three-phase three-wire converter under the unbalanced ac source

$$Q_{c2} = 0$$

$$Q_{s2} = 0 \tag{17}$$

$$P_{c2} = 0$$

$$Q_{s2} = 0 \tag{18}$$

$$P_{s2} = 0$$

$$Q_{c2} = 0. \tag{19}$$

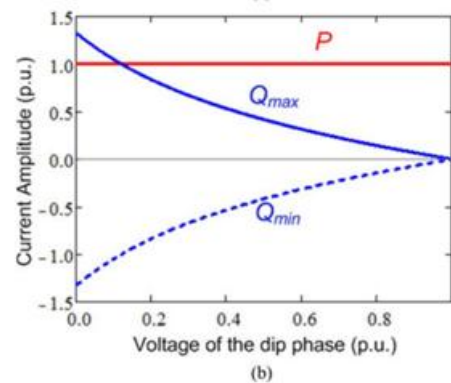
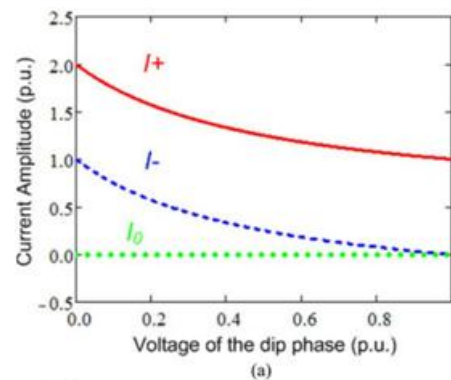


Fig. 8. Profile of converter control with no active power oscillation (three-phase three-wire converter, Pref = 1 p.u., Qref = 0 p.u., Ps2 = 0 p.u., Pc2 = 0 p.u.). (a) Sequence current amplitude versus VA . (I+, I-, and I0 means the amplitude of the current in the positive, negative, and zero sequences, respectively). (b) P and Q range versus VA .

III. CONVERTER SYSTEM WITH THE ZERO-SEQUENCE CURRENT PATH

As can be concluded, in the typical three-phase three-wire converter structure, four control freedoms for the load current seem to be not enough to achieve

satisfactory performances under the unbalanced ac source. (No matter what combinations of control targets are used, either significant power oscillation or overloaded/distorted current will be presented.) Therefore, more current control freedoms are needed in order to improve the control performance under the unbalanced ac source conditions. Another series of the converter structure are shown as indicated as the four-wire system in Fig. 9(a) and the six-wire system in Fig. 9(b). Compared to the three-wire converter structure, these types of converters introduce the zero-sequence current path [24]–[26], which may enable extra current control freedoms to achieve better power control performances. It is noted that in the grid-connected application, the zero-sequence current is not injected into the grid but trapped in the typically used d - Y transformer.

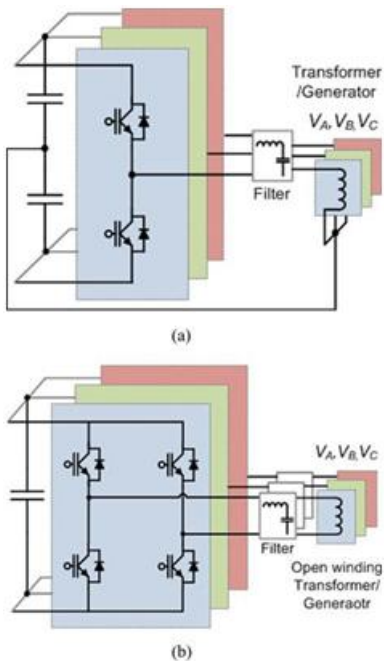


Fig. 9. Converter structure with the zero-sequence current path. (a) Four-wire system. (b) Six-wire system

A potential control structure is proposed in Fig. 10, in which an extra control loop is introduced to enable the controllability of the zero-sequence current. After introducing the regulated zero-sequence current, the three-phase current generated by the converter can be written as [27]–[29]

By operating the voltage of the ac source (1) and the current controlled by the power converter (20), the instantaneous generated real power p , the imaginary power q in the $\alpha\beta$ coordinate, and the real power p_0 in the zero coordinate can be calculated as

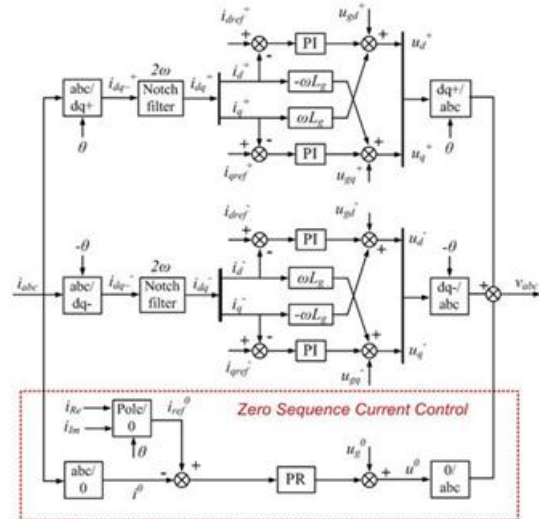


Fig. 10. Control structure for the converter system with the zero-sequence current

$$I_C = I^+ + I^- + I^0. \quad (20)$$

$$\begin{bmatrix} p \\ q \\ p_0 \end{bmatrix} = \begin{bmatrix} v_\alpha \cdot i_\alpha + v_\beta \cdot i_\beta \\ v_\alpha \cdot i_\beta - v_\beta \cdot i_\alpha \\ v_0 \cdot i_0 \end{bmatrix} = \begin{bmatrix} \bar{P} + P_{e2} \cdot \cos(2\omega t) + P_{s2} \cdot \sin(2\omega t) \\ \bar{Q} + Q_{e2} \cdot \cos(2\omega t) + Q_{s2} \cdot \sin(2\omega t) \\ \bar{P}_0 + P_{0e2} \cdot \cos(2\omega t) + P_{0s2} \cdot \sin(2\omega t) \end{bmatrix}. \quad (21)$$

Then, the instantaneous three-phase real power $p_{3\phi}$ and the imaginary power $q_{3\phi}$ of the converter can be written as

$$\begin{bmatrix} p_{3\phi} \\ q_{3\phi} \end{bmatrix} = \begin{bmatrix} p + p_0 \\ q \end{bmatrix} = \begin{bmatrix} \bar{P} + \bar{P}_0 \\ \bar{Q} \end{bmatrix} + \begin{bmatrix} P_{e2} + P_{0e2} \\ Q_{e2} \end{bmatrix} \cos(2\omega t) + \begin{bmatrix} P_{s2} + P_{0s2} \\ Q_{s2} \end{bmatrix} \sin(2\omega t). \quad (22)$$

It is noted that the voltage and the current in zero sequence only contribute to the real power $p_{3\phi}$ of the converter. Each part of (22) can be calculated as

$$\begin{aligned} \bar{P} &= \frac{3}{2}(v_d^+ \cdot i_d^+ + v_q^+ \cdot i_q^+ + v_d^- \cdot i_d^- + v_q^- \cdot i_q^-) \\ P_{c2} &= \frac{3}{2}(v_d^- \cdot i_d^+ + v_q^- \cdot i_q^+ + v_d^+ \cdot i_d^- + v_q^+ \cdot i_q^-) \\ P_{s2} &= \frac{3}{2}(v_q^- \cdot i_d^+ - v_d^- \cdot i_q^+ - v_q^+ \cdot i_d^- + v_d^+ \cdot i_q^-) \end{aligned} \quad (23)$$

$$\begin{aligned} \bar{Q} &= \frac{3}{2}(v_d^+ \cdot i_d^+ - v_d^- \cdot i_q^+ + v_q^- \cdot i_d^- - v_q^+ \cdot i_q^-) \\ Q_{c2} &= \frac{3}{2}(v_q^- \cdot i_d^+ - v_d^- \cdot i_q^+ + v_d^+ \cdot i_d^- - v_d^+ \cdot i_q^-) \\ Q_{s2} &= \frac{3}{2}(-v_d^- \cdot i_d^+ - v_q^- \cdot i_q^+ + v_d^+ \cdot i_d^- + v_q^+ \cdot i_q^-) \end{aligned} \quad (24)$$

$$\begin{aligned} \bar{P}_0 &= \frac{3}{2}(v_{Re}^0 \cdot i_{Re}^0 + v_{Im}^0 \cdot i_{Im}^0) \\ P_{0c2} &= \frac{3}{2}(v_{Re}^0 \cdot i_{Re}^0 - v_{Im}^0 \cdot i_{Im}^0) \\ P_{0s2} &= \frac{3}{2}(-v_{Im}^0 \cdot i_{Re}^0 - v_{Re}^0 \cdot i_{Im}^0). \end{aligned} \quad (25)$$

Then, the relationship of (23)–(25) can be formulated to a matrix equation as

$$\begin{bmatrix} \bar{P} + \bar{P}_0 \\ P_{c2} + P_{0c2} \\ P_{s2} + P_{0s2} \\ \bar{Q} \\ Q_{c2} \\ Q_{s2} \end{bmatrix} = \frac{3}{2} \begin{bmatrix} v_d^+ & v_q^+ & v_d^- & v_q^- & v_{Re}^0 & v_{Im}^0 \\ v_d^- & v_q^- & v_d^+ & v_q^+ & v_{Re}^0 & -v_{Im}^0 \\ v_q^- & -v_d^- & -v_q^+ & v_d^+ & -v_{Im}^0 & -v_{Re}^0 \\ v_q^+ & -v_d^+ & v_q^- & -v_d^- & 0 & 0 \\ v_q^- & -v_d^- & v_q^+ & -v_d^+ & 0 & 0 \\ -v_d^- & -v_q^- & v_d^+ & v_q^+ & 0 & 0 \end{bmatrix} \begin{bmatrix} i_d^+ \\ i_q^+ \\ i_d^- \\ i_q^- \\ i_{Re}^0 \\ i_{Im}^0 \end{bmatrix} \quad (26)$$

It is noted that unlike the traditional approach in which the zero sequence components are normally minimized, the zero sequence voltage and the current here look like single-phase AC components running at the same fundamental frequency. As a result, the zero-sequence voltage/current can be represented by vectors in a synchronous reference frame in the zero sequence as

$$\begin{aligned} \mathbf{V}_0 &= v_{Re}^0 + v_{Im}^0 j \\ \mathbf{I}_0 &= i_{Re}^0 + i_{Im}^0 j \end{aligned} \quad (27)$$

where the real part and imaginary part can be represented as follows:

$$\begin{aligned} v_{Re}^0 &= V^0 \cos(\varphi^0) \\ v_{Im}^0 &= V^0 \sin(\varphi^0) \\ i_{Re}^0 &= I^0 \cos(\delta^0) \\ i_{Im}^0 &= I^0 \sin(\delta^0). \end{aligned} \quad (28)$$

It can be seen from (26) that if the three-phase ac source voltage is decided, then the converter has six controllable freedoms ($i_d^+, i_q^+, i_d^-, i_q^-, i_{Re}^0$, and i_{Im}^0) to regulate the current flowing in the ac source. That means: six control targets/functions can be established by the converter having the zero-sequence current path. Similarly, the three-phase average active and reactive power delivered by the converter are two basic requirements for a given application, then, two control functions need to be first settled as

$$\begin{aligned} \overline{P_{3\phi}} &= \bar{P} + \bar{P}_0 = P_{ref} \\ \overline{Q_{3\phi}} &= \bar{Q} = Q_{ref}. \end{aligned} \quad (29)$$

So, for the converter system with the zero-sequence current path, there are four control freedoms left to achieve two more control targets than the traditional three-wire system, this also means extended controllability and better performance under the unbalanced ac source.

A. Elimination of Both the Active and Reactive Power Oscillation.

Because of more current control freedoms, the power converter with the zero-sequence current path can not only eliminate the oscillation in the active power, but also cancel the oscillation in the reactive power at the same time. This control targets can be written as

$$\begin{aligned} P_{3\phi c2} &= P_{c2} + P_{0c2} = 0 \\ P_{3\phi s2} &= P_{s2} + P_{0s2} = 0 \\ Q_{c2} &= 0 \\ Q_{s2} &= 0. \end{aligned} \quad (30)$$

The power oscillation caused by the zero-sequence current P_{0c2} and P_{0s2} are used to compensate the power oscillation caused by the positive- and negative-sequence currents P_{c2} and P_{s2} .

When combing (26), (30), and (31), each of the current components controlled by converter can be calculated as

$$\begin{bmatrix} i_d^+ \\ i_q^+ \\ i_d^- \\ i_q^- \\ i_{Re}^0 \\ i_{Im}^0 \end{bmatrix} = \frac{2}{3} \begin{bmatrix} v_d^+ & v_q^+ & v_d^- & v_q^- & v_{Re}^0 & v_{Im}^0 \\ v_d^- & v_q^- & v_d^+ & v_q^+ & v_{Re}^0 & -v_{Im}^0 \\ v_q^- & -v_d^- & -v_q^+ & v_d^+ & -v_{Im}^0 & -v_{Re}^0 \\ v_q^+ & -v_d^+ & v_q^- & -v_d^- & 0 & 0 \\ v_q^- & -v_d^- & v_q^+ & -v_d^+ & 0 & 0 \\ -v_d^- & -v_q^- & v_d^+ & v_q^+ & 0 & 0 \end{bmatrix}^{-1} \begin{bmatrix} P_{ref} \\ 0 \\ 0 \\ Q_{ref} \\ 0 \\ 0 \end{bmatrix} \quad (32)$$

In order to facilitate the analytical solution, assuming that the d -axis or the real axis in the synchronous reference frame is allied with the voltage vectors in each of the sequence (pos-itive, negative, and zero), then all of the controllable current components with the zero-sequence current path can be solved By

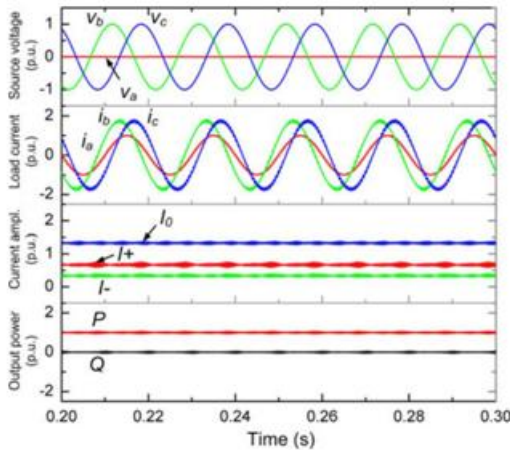


Fig. 11. Simulation of converter control with no active and reactive power oscillation (three-phase converter with the zero-sequence path, $P_{ref} = 1$ p.u., $Q_{ref} = 0$ p.u., $P_{s2} = 0$ p.u., $P_{c2} = 0$ p.u., $Q_{s2} = 0$ p.u., $Q_{c2} = 0$ p.u., $V_A = 0$ p.u.).

$$i_d^+ \approx \frac{2}{3} \cdot \frac{P_{ref}}{(v_d^+ - v_d^-) \cdot (1 - v_d^-/v_d^+)}$$

$$i_q^+ \approx \frac{2}{3} \cdot \frac{Q_{ref}}{-v_d^+ + (v_d^-)^2/v_d^+} \quad (33)$$

$$i_d^- \approx \frac{v_d^-}{v_d^+} \cdot i_d^+$$

$$i_q^- \approx -\frac{v_d^-}{v_d^+} \cdot i_q^+ \quad (34)$$

$$i_{Re}^0 \approx \frac{2}{3} \cdot \frac{P_{ref} - \bar{P}}{v_{Re}^0}$$

$$i_{Im}^0 \approx \frac{v_d^+ \cdot i_q^- - v_d^- \cdot i_q^+}{v_{Re}^0} \quad (35)$$

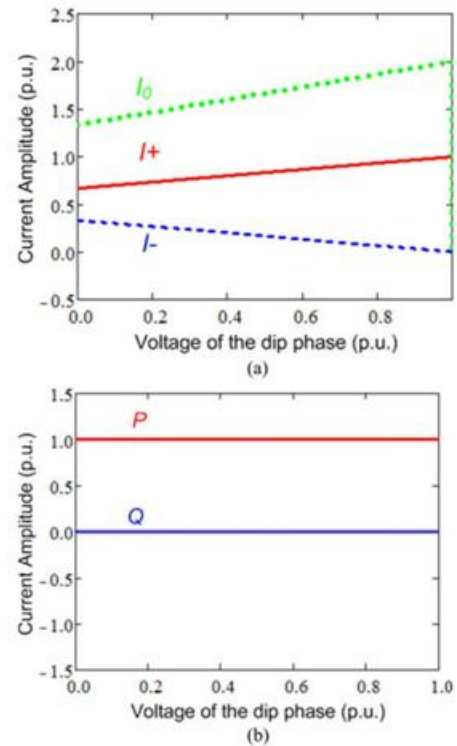


Fig. 12. Profile of converter control with no active and reactive power oscillation (three-phase converter with the zero sequence path, $P_{ref} = 1$ p.u., $Q_{ref} = 0$ p.u., $P_{s2} = 0$ p.u., $P_{c2} = 0$ p.u., $Q_{s2} = 0$ p.u., $Q_{c2} = 0$ p.u.). (a) Sequence current amplitude versus V_A . (I_+ , I_- , and I_0 means the amplitude of the current in the positive, negative, and zero sequences, respectively). (b) P and Q ranges versus V_A

When applying the current references in (33)–(35), the corresponding ac source voltage, load current, sequence current, and the instantaneous power delivered by the converter are shown in Fig. 11. It can be seen that by this control strategy, the oscillation of both the active and reactive power at twice of the fundamental frequency can be eliminated. Moreover, compared to the control strategies for the three-wire system, the amplitude of the load current in each phase is not further increased, and the current in the faulty phase is smaller than the other two normal phases—this is a significant improvement. The current amplitude in different sequences, as well as the delivered active/reactive power with relation to the voltage amplitude on the dipping phase is shown in Fig. 12(a) and (b), respectively. It is noted that the converter has to deliver positive-, negative-, and zero-sequence currents to achieve this control strategy. And the zero sequence current is controlled as zero when the voltage dip is at 1.0 p.u.

B. Elimination of the Active Power Oscillation and the Negative-Sequence Current.

Another promising control strategy for the converter using the zero-sequence current path is to eliminate the active power oscillation, and meanwhile cancel the negative-sequence current. The extra two control targets besides (26) can be written

$$\begin{aligned} P_{3\phi c2} &= P_{c2} + P_{0c2} = 0 \\ P_{3\phi s2} &= P_{s2} + P_{0s2} = 0 \end{aligned} \quad (36)$$

$$\begin{aligned} i_d^- &= 0 \\ i_q^- &= 0. \end{aligned} \quad (37)$$

Combining (26), (36), and (37), the matrix equation of (26) can be degraded as

$$\begin{bmatrix} \bar{P} + \bar{P}_0 \\ P_{c2} + P_{0c2} \\ P_{s2} + P_{0s2} \\ \bar{Q} \end{bmatrix} = \frac{3}{2} \begin{bmatrix} v_d^+ & v_q^+ & v_{Re}^0 & v_{Im}^0 \\ v_d^- & v_q^- & v_{Re}^0 & -v_{Im}^0 \\ v_q^- & -v_d^- & -v_{Im}^0 & -v_{Re}^0 \\ v_q^+ & -v_d^+ & 0 & 0 \end{bmatrix} \begin{bmatrix} i_d^+ \\ i_q^+ \\ i_{Re}^0 \\ i_{Im}^0 \end{bmatrix} \quad (38)$$

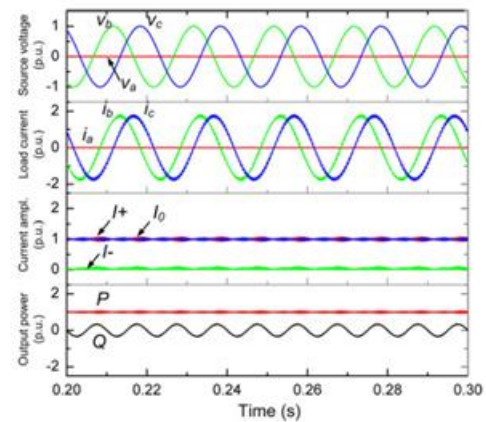


Fig. 13. Simulation of converter control with no active power oscillation and no negative sequence (three-phase converter with the zero-sequence current path, $P_{ref} = 1$ p.u., $Q_{ref} = 0$ p.u., $P_{s2} = 0$ p.u., $P_{c2} = 0$ p.u., $i_{d-} = 0$ p.u., $i_{q-} = 0$ p.u., $V_A = 0$ p.u. I^+, I^- , and I_0 means the amplitude of the current in the positive, negative, and zero sequences, respectively).

And each of the current components can be calculated as

$$\begin{bmatrix} i_d^+ \\ i_q^+ \\ i_{Re}^0 \\ i_{Im}^0 \end{bmatrix} = \frac{2}{3} \begin{bmatrix} v_d^+ & v_q^+ & v_{Re}^0 & v_{Im}^0 \\ v_d^- & v_q^- & v_{Re}^0 & -v_{Im}^0 \\ v_q^- & -v_d^- & -v_{Im}^0 & -v_{Re}^0 \\ v_q^+ & -v_d^+ & 0 & 0 \end{bmatrix}^{-1} \begin{bmatrix} P_{ref} \\ 0 \\ 0 \\ Q_{ref} \end{bmatrix} \quad (39)$$

In order to facilitate the analytical solution, assuming that the d-axis or the real axis in the synchronous reference frame is allied with the voltage vectors in each of the sequence, then all of the controllable current components with the zero-sequence current path can be solved as

$$\begin{aligned} i_d^+ &\approx \frac{2}{3} \cdot \frac{P_{ref}}{(v_d^+ - v_d^-)} \\ i_q^+ &\approx \frac{2}{3} \cdot \frac{Q_{ref}}{-v_d^+} \end{aligned} \quad (40)$$

$$\begin{aligned} i_d^- &= 0 \\ i_q^- &= 0 \end{aligned} \quad (41)$$

$$\begin{aligned} i_{Re}^0 &\approx \frac{-v_d^- \cdot i_d^+}{v_{Re}^0} \\ i_{Im}^0 &\approx 0. \end{aligned} \quad (42)$$

When applying the current references in (40)–(42), the corresponding source voltage, load current, sequence current, and the instantaneous power delivered by converter are shown in Fig. 13. It can be seen that by this control strategy, the oscillation of the active power at twice of the fundamental frequency can be eliminated, and the load current in the faulty phase is reduced to zero. The current amplitude in the different sequences, as well as the delivered active/reactive power with relation to the voltage.

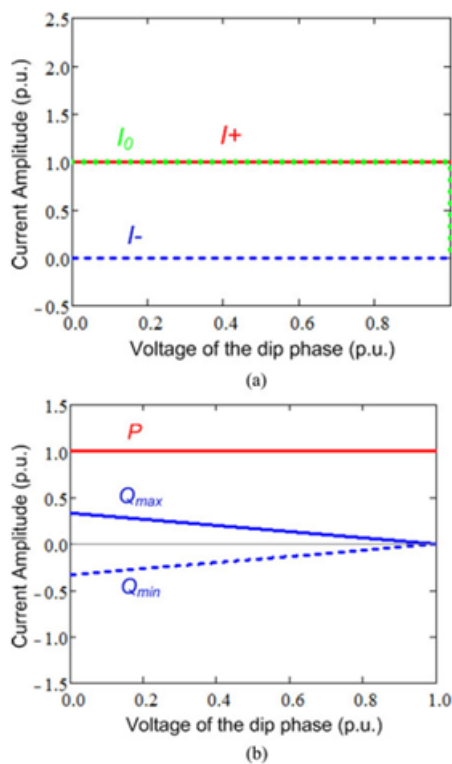


Fig. 14. Profile of converter control with no active power oscillation and no negative sequence (three-phase converter with the zero-sequence current path, $P_{ref} = 1$ p.u., $Q_{ref} = 0$ p.u., $P_{s2} = 0$ p.u., $P_{c2} = 0$ p.u., $i_{d-} = 0$ p.u., $i_{q-} = 0$ p.u.). (a) Sequence current amplitude versus V_A . (b) P and Q ranges versus V_A .

Age on the dipping phase are shown in Fig. 14(a) and (b), respectively. It is noted that the converter has to deliver constant positive- and zero-sequence currents in order to achieve this control strategy under different dips of the source voltage.

The oscillation of the reactive power is maintained in a much smaller range (up to ± 0.3 p.u.) compared to that in the three-wire system (up to ± 1.3 p.u.) in Fig. 8(b). The zero-sequence current is controlled as zero when the voltage dip is at 1.0 p.u. Finally, the converter stresses for the active/reactive power oscillations and the current amplitude in the faulty/normal phases are compared in Table II, where different control strategies and converter structures are indicated, respectively. It can be seen that by introducing the converter structures with the zero sequence current path and corresponding controls, the power oscillations under the unbalanced ac source are significantly reduced; meanwhile, the current amplitude in the normal phases is not further stressed, and the current stress in the faulty phases is significantly relieved. It is worth to mention that when enabling the proposed control methods, the zero-sequence current is flowing in/out of the midpoint of the dc bus at the fundamental frequency, there by

TABLE II
CONVERTER STRESS COMPARISON BY DIFFERENT CONTROL STRATEGIES
(VALUES ARE REPRESENTED IN p.u., $P_{ref} = 1$ p.u., $Q_{ref} = 0$ p.u., AND $V_A = 0$ p.u.)

Converter stress	Typical 3-wire		Zero-sequence	
	Control A	Control B	Control A	Control B
Active power osc. P_{osc}	0.5	0	0	0
Reactive power osc. Q_{osc}	0.5	1.3	0	0.3
Current in faulty phase I_{fault}	1.5	3	1	0
Current in normal phase I_{norm}	1.5	2	2	2

Typical three-wire converter.
 Control A: no negative-sequence current.
 Control B: no active power oscillation.
 Converter with the zero-sequence current path.
 Control A: no active and reactive power oscillations.
 Control B: no active power oscillation and no negative-sequence current.

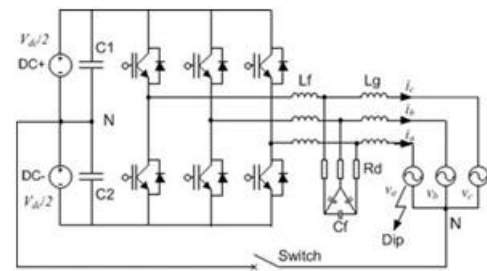
A larger dc capacitance or a rectifier with controllability of the midpoint potential is preferred for the four-wire converter structure shown in Fig. 9(a). However, there is no such problem in the six-wire converter structure shown in Fig. 9(b). Moreover, according to (35) and (42), the reference current for the zero sequence is inverse proportional with the zero sequence voltage v_0 . The effectiveness of the proposed control methods should rely on the amount of v_0 in the unbalanced ac source. In some cases of two-phase or three-phase faults with no or very small v_0 , the performance of the proposed control strategies will be different, and new control methods which do not utilize the power from the zero sequence are needed.

It is also noted that the dynamical performance and the sequence-extracting algorithm are also critical considerations for the control methods under the unbalanced ac source, either for the transient condition (e.g., LVRT) or the stability during the steady-state operation, however, they are out of the scope of this paper.

IV. EXPERIMENTAL RESULTS:

The control results by different converter structures and control strategies are validated on a downscale dc-ac converter. As shown in Fig. 15, the circuit configurations and setup photo are both illustrated. A three-phase two-level converter with corresponding LCL filter is used to interconnect two dc voltage sources and a programmable three-phase ac voltage source. The detail parameters of the experimental setup are shown in Table III. It is noted that the converter is controlled to operate at the inverter mode, where the active power is flowing from the dc source to the ac source. By opening and closing a switch shown in Fig. 15(a), the converter can be shifted between the typical three-wire system and four-wire system with the zero-sequence current path.

The amplitude of the phase A voltage in the programmable ac source is adjusted to 0.1 p.u. ($22 V_{rms}$) in order to establish an adverse unbalanced condition. The control performance of the converter with the three-wire structure are shown in Fig. 16, where the given conditions and the two control strategies mentioned in Figs. 5 and 7 are applied, respectively. It can be seen that the experimental results agree well with the analysis and simulation results, where either the significant power oscillations or the overloaded current in the faulty phase are presented.



(a)



(b)

Fig. 15. Configurations of the experimental setup. (a) Circuit topology (b) Setup photo.

TABLE III: DETAIL PARAMETERS OF THE EXPERIMENTAL SETUP

DC bus voltage V_{dc}	700 V DC
DC capacitance C_1/C_2	3300 μ F
Nominal power P_{norm}	5.5 kW
Nominal AC voltage V_{norm}	311 V
Nominal load current I_{norm}	11.8 A
Fundamental frequency f_o	50 Hz
Switching frequency f_s	20 kHz
Filter inductance L_f	11 mH
AC source side inductance L_g	7.3 mH
Filter capacitance C_f	2.2 μ F
Damping resistance R_d	3.5 Ω

After enabling the zero current path and proposed controls, the performances of the given converter are shown again in Fig. 17, where the same conditions and two control strategies mentioned in Figs. 11 and 13 are applied, respectively. It can be seen that the experimental results also agree well with the simulation results, where the power oscillations are much more reduced or even totally cancelled; meanwhile, the current stress in the faulty phase is significantly relieved. These critical performances are hard to be achieved by a single three-wire converter structure using existing control strategies.

The capability to control the reactive power is also a critical performance for the converter under the unbalanced ac source, the proposed two control methods are also tested under the conditions to deliver the inductive/capacitive reactive power. As shown in Figs. 18 and 19, the *No P & No Q oscillation control* and *No negative-sequence current & No P oscillation control* are applied, respectively, to deliver the inductive and capacitive reactive power with phase A voltage dipping to 0.5 p.u. It can be seen that the advantages of the smaller/eliminated power oscillation and the relieved current loading in the faulty phase

reference given: $P_{ref} = 0.5$ p.u., $Q_{ref} = 0$ p.u., ac source condition: amplitude of the phase voltage $V_A = 0.1$ p.u., $V_B = V_C = 1$ p.u.). (a) No negative-sequence current control (b) No P oscillation control.

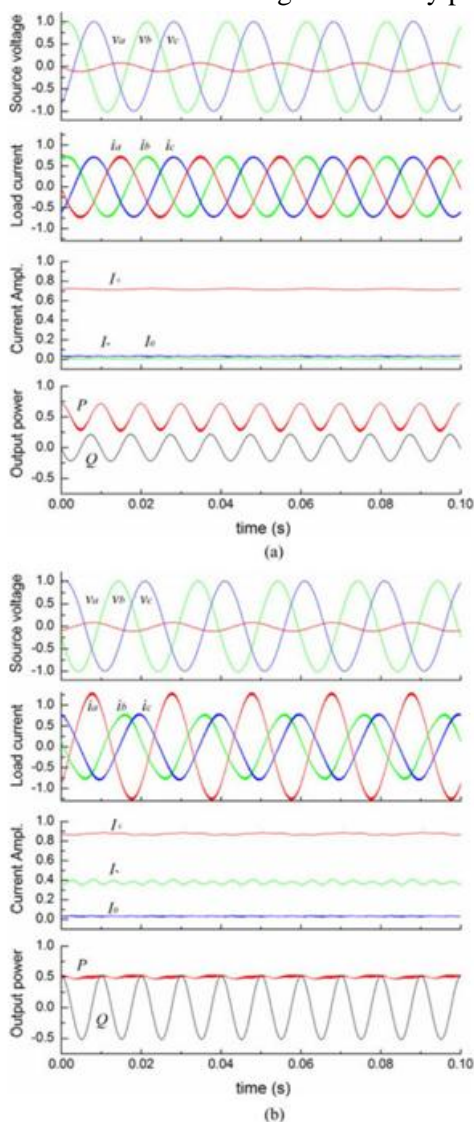


Fig. 16. Experimental control performance of the converter in Fig. 15(a) with only three wires (units are nominalized by parameters in Table III,

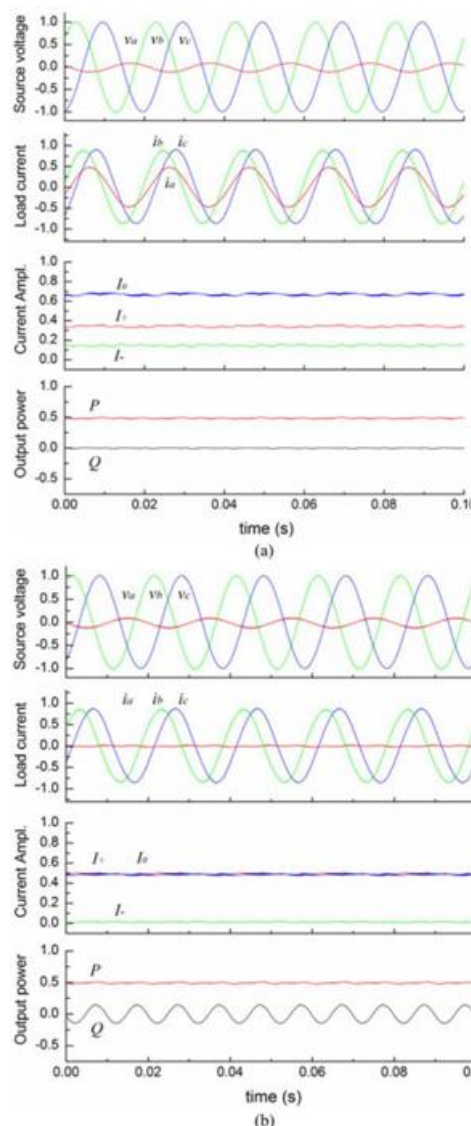
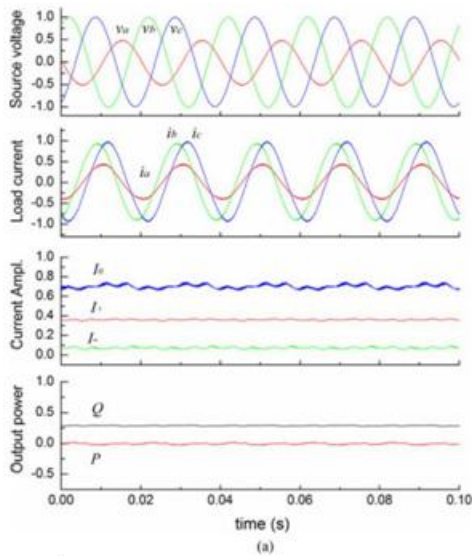
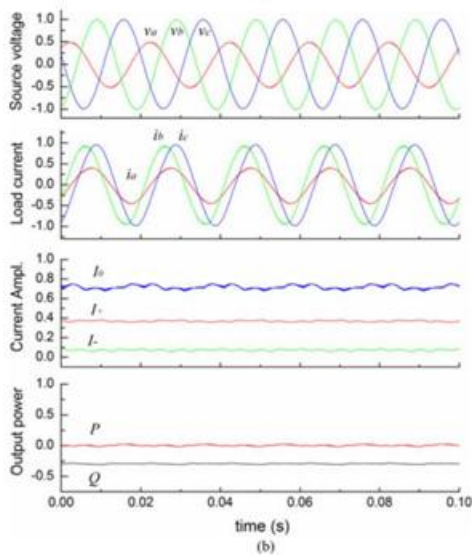


Fig. 17. Experimental control performance of the converter in Fig. 15(a) after enabling the zero-sequence current path (units are nominalized by parameters in Table III, reference given: $P_{ref} = 0.5$ p.u., $Q_{ref} = 0$ p.u., amplitude of the phase voltage $V_A = 0.1$ p.u., $V_B = V_C = 1$ p.u.). (a) No P and no Q oscillation control (b) No negative-sequence current and no P oscillation control.

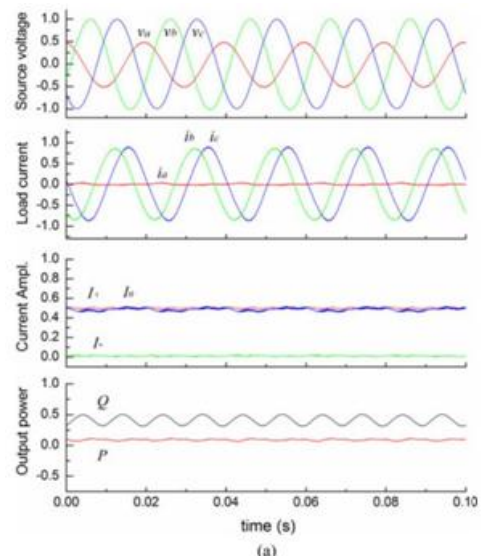


(a)

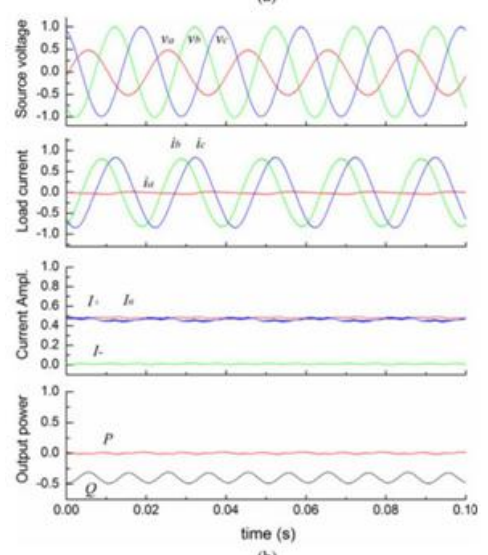


(b)

Fig. 18. Experimental results of the converter's reactive power capability when using no P & no Q oscillation control in Fig. 17(a). (units are nominalized by parameters in Table III, reference given: $P_{ref} = 0$ p.u., $Q_{ref} \approx \pm 0.25$ p.u. when the maximum load current achieves 1 p.u., the amplitude of the phase voltage $V_A = 0.5$ p.u., $V_B = V_C = 1$ p.u.). (a) Deliver inductive reactive power ($Q+$). (b) Deliver capacitive reactive power ($Q-$).



(a)



(b)

Fig. 19. Experimental results of the converter's reactive power capability when using no negative-sequence current and no P oscillation control shown in Fig. 17(b). (units are nominalized by parameters in Table III, reference given: $P_{ref} = 0$ p.u., $Q_{ref} \approx \pm 0.5$ p.u. when the maximum load current achieves 1 p.u., the amplitude of the phase voltage $V_A = 0.5$ p.u., $V_B = V_C = 1$ p.u.). (a) Deliver inductive reactive power ($Q+$). (b) Deliver capacitive reactive power ($Q-$).

V. CONCLUSION:

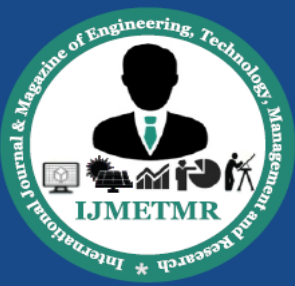
In a typical three-phase three-wire converter structure, there are four current control freedoms, and it may be not enough to achieve satisfactory performances under

the unbalanced ac source, because either significantly the oscillated power or the overloaded current will be presented. In the three-phase converter structure with the zero sequence current path, there are six current control freedoms. The extra two control freedoms coming from the zero sequence current can be utilized to extend the controllability of the converter and improve the control performance under the unbalanced ac source. By the proposed control strategies, it is possible to totally cancel the oscillation in both the active and the reactive power, or reduced the oscillation amplitude in the reactive power. Meanwhile, the current amplitude of the faulty phase is significantly relieved without further increasing the current amplitude in the normal phases. The advantage and features of the proposed controls can be still maintained under various conditions when delivering the reactive power. The analysis and proposed control methods are well agreed by experimental validation.

REFERENCES:

- [1] F. Blaabjerg, M. Liserre, and K. Ma, "Power electronics converters for wind turbine systems," *IEEE Trans. Ind. Appl.*, vol. 48, no. 2, pp. 708–719, Mar./Apr. 2012.
- [2] R. Teodorescu, M. Liserre, and P. Rodriguez, *Grid Converters for Photovoltaic and Wind Power Systems*. New York, NY, USA: Wiley-IEEE, 2011.
- [3] J. Rocabert, G. M. S. Azevedo, A. Luna, J. M. Guerrero, J. I. Candela, and P. Rodriguez, "Intelligent connection agent for three-phase grid-connected microgrids," *IEEE Trans. Power Electron.*, vol. 26, no. 10, pp. 2993–3005, Oct. 2011.
- [4] J. W. Kolar and T. Friedli, "The essence of three-phase PFC rectifier systems—Part I," *IEEE Trans. Power Electron.*, vol. 28, no. 1, pp. 176–198, Jan. 2013.
- [5] J. Hu, L. Shang, Y. He, and Z. Z. Zhu, "Direct active and reactive power regulation of grid-connected dc/ac converters using sliding mode control approach," *IEEE Trans. Power Electron.*, vol. 26, no. 1, pp. 210–222, Jan. 2011.
- [6] C. Wessels, F. Gebhardt, and F. W. Fuchs, "Fault ride-through of a DFIG wind turbine using a dynamic voltage restorer during symmetrical and asymmetrical grid faults," *IEEE Trans. Power Electron.*, vol. 26, no. 3, pp. 807–815, Mar. 2011.
- [7] F. Aghili, "Fault-tolerant torque control of BLDC motors," *IEEE Trans. Power Electron.*, vol. 26, no. 2, pp. 355–363, Feb. 2011.
- [8] Y. Xiangwu, G. Venkataramanan, W. Yang, D. Qing, and Z. Bo, "Grid-fault tolerant operation of a DFIG wind turbine generator using a passive resistance network," *IEEE Trans. Power Electron.*, vol. 26, no. 10, pp. 2896–2905, Oct. 2011.
- [9] B. A. Welchko, T. A. Lipo, T. M. Jahns, and S. E. Schulz, "Fault tolerant three-phase AC motor drive topologies: A comparison of features, cost, and limitations," *IEEE Trans. Power Electron.*, vol. 19, no. 4, pp. 1108–1116, Jul. 2004.
- [10] F. Blaabjerg, K. Ma, and D. Zhou, "Power electronics and reliability in renewable energy systems," in *Proc. IEEE Int. Symp. Ind. Electron.*, May 2012, pp. 19–30.
- [11] Y. Song and B. Wang, "Survey on reliability of power electronic systems," *IEEE Trans. Power Electron.*, vol. 28, no. 1, pp. 591–604, Jan. 2013.
- [12] M. Altin, O. Goksu, R. Teodorescu, P. Rodriguez, B. Bak-Jensen, and L. Helle, "Overview of recent grid codes for wind power integration," in *Proc. 12th Int. Conf. Optim. Elect. Electron. Equip.*, 2010, pp. 1152–1160.

- [13] Grid Code. High and Extra High Voltage, E.ON-netz, Bayreuth, Germany, Apr. 2006.
- [14] P. Rodr'iguez, A. Luna, R. Munoz~Aguilar, I. Etxeberria-Otadui, R. Teodorescu, and F. Blaabjerg, "A stationary reference frame grid synchronization system for three-phase grid-connected power converters un-der adverse grid conditions," *IEEE Trans. Power Electron.*, vol. 27, no. 1, pp. 99–112, Jan. 2012.
- [15] A. J. Roscoe, S. J. Finney, and G. M. Burt, "Tradeoffs between AC power quality and DC bus ripple for 3-phase 3-wire inverter-connected devices within microgrids," *IEEE Trans. Power Electron.*, vol. 26, no. 3, pp. 674– 688, Mar. 2011.
- [16] C. H. Ng, Li Ran, and J. Bumby, "Unbalanced-grid-fault ride-through control for a wind turbine inverter," *IEEE Trans. Ind. Appl.*, vol. 44, no. 3, pp. 845–856, May/June. 2008.
- [17] P. Rodriguez, A. V. Timbus, R. Teodorescu, M. Liserre, and F. Blaabjerg, "Flexible active power control of distributed power generation systems during grid faults," *IEEE Trans. Ind. Electron.*, vol. 54, no. 5, pp. 2583– 2592, Oct. 2007.
- [18] H. Song and K. Nam, "Dual current control scheme for PWM converter under unbalanced input voltage conditions," *IEEE Trans. Ind. Electron.*, vol. 46, no. 5, pp. 953–959, Oct. 1999.
- [19] H. Akagi, Y. Kanazawa, and A. Nabae, "Instantaneous reactive power compensators comprising switching devices without energy storage com-ponents," *IEEE Trans. Ind. Appl.*, vol. IA-20, no. 3, pp. 625–630, May 1984.
- [20] J. Miret, M. Castilla, A. Camacho, L. Vicuna,~ and J. Matas, "Control scheme for photovoltaic three-phase inverters to minimize peak cur-rents during unbalanced grid-voltage sags," *IEEE Trans. Power Electron.*, vol. 27, no. 10, pp. 4262–4271, Oct. 2012.
- [21] F. Gonzalez'-Esp'ın, G. Garcera,' I. Patrao, and E. Figueres, "An adaptive control system for three-phase photovoltaic inverters working in a pol-luted and variable frequency electric grid," *IEEE Trans. Power Electron.*, vol. 27, no. 10, pp. 4248–4261, Oct. 2012.
- [22] G. Saccomando, J. Svensson, and A. Sannino, "Improving voltage dis-turbance rejection for variable-speed wind turbines," *IEEE Trans. Energy Convers.*, vol. 17, no. 3, pp. 422–428, Sep. 2002.
- [23] N. Kaminski and A. Kopta, "Failure rates of HiPak Modules due to cosmic rays," ABB Switzerland Ltd., Zurich, Switzerland, ABB Appl. note 5SYA 2042-04, Mar. 2011.
- [24] S. Sharma and B. Singh, "Performance of voltage and frequency controller in isolated wind power generation for a three-phase four-wire system," *IEEE Trans. Power Electron.*, vol. 26, no. 12, pp. 3443–3452, Dec. 2011.
- [25] K. Ma, F. Blaabjerg, and M. Liserre, "Thermal analysis of multilevel grid side converters for 10 mw wind turbines under low voltage ride through," *IEEE Trans. Ind. Appl.*, vol. 49, no. 2, pp. 909–921, Mar./Apr. 2013.
- [26] J. Holtz and N. Oikonomou, "Optimal control of a dual three-level inverter system for medium-voltage drives," *IEEE Trans. Ind. Appl.*, vol. 46, no. 3, pp. 1034–1041, May/June. 2010.
- [27] E. H. Watanabe, R. M. Stephan, and M. Aredes, "New concepts of in-stantaneous active and reactive powers in electrical systems with



generic loads,” IEEE Trans. Power Del., vol. 8, no. 2, pp. 697–703, Apr. 1993.

strategies,” IEEE Trans. Power Electron., vol. 12, no. 2, pp. 311–318, Mar. 1997.

[28] M. Aredes and E. H. Watanabe, “New control algorithms for series and shunt three-phase four-wire active power filters,” IEEE Trans. Power Del., vol. 10, no. 3, pp. 1649–1656, Jul. 1995.

[30] C.-T. Lee, C.-W. Hsu, and P.-T. Cheng, “A low-voltage ride-through technique for grid-connected converters of distributed energy resources,” IEEE Trans. Ind. Appl., vol. 47, no. 4, pp. 1821–1832, Jul./Aug. 2011.

[29] M. Aredes, J. Hafner, and K. Heumann, “Three-phase four-wire shunt active filter control